

Generation of Iron Nano-microparticles for Bio-medical Applications Using Plasma Processes

MADALIN BUNOIU¹, EUGEN MIRCEA ANTIAS^{2,3*}, JOHNY NEAMTU⁴, IOAN BICA¹, LIVIU CHIRIGIU⁴, LARISA MARINA ELIZABETH CHIRIGIU⁴

¹West University of Timisoara, 4 Vasile Parvan Blvd, 300223, Timisoara, Romania

²Joint Institute for Nuclear Research, Dubna, Russia

³Horia Hulubei National Institute of Physics and Nuclear Engineering, 30 Reactorului Str., Bucharest-Magurele, Romania

⁴University of Medicine and Pharmacy Craiova, 2 Petru Rares Str., 200349, Craiova, Romania

In the last years, experimental diagnosis and therapy for cancer patients is performed using nano-micro technologies, and in particular iron nano-microparticles since their ad/absorbance properties, are useful in transporting and maintaining drugs in tumor regions. In this paper, a plasma generation process is used for spraying solid metal (carbon steel wire or rod). By modifying the electric current intensity, material's displacement speed in plasma and the debit of technical argon, iron nano-microparticles are obtained in the form of filled and/or porous microspheres, nano-microtubes and microparticles. They consist of a central core from which tentacles in the form of microtubes emerge. We show the manufacturing process and the formation mechanisms of these particles by using argon plasma. We present and discuss the obtained results.

Keywords: nano-microparticles, plasma generator, magnetic field, nano-microtubes

The processes of generating fine and ultrafine particles can be divided into two main groups: chemical and physical methods. Chemical methods [1] are based on the co-precipitation of metal compounds (oxides, organometallics etc.) in proper environments, followed by the formation of particles dispersed in a liquid matrix [2]. Physical methods [3] are based on solid metal evaporation in plasma arc [4, 5], tungsten-inert gas (TIG) arc, metal-inert gas (MIG) arc [6], thermal decomposition of organometallics [7, 8], spraying the metals in plasma jet [9] etc. The reaction products condense on the atoms or molecules of the gas, and particles of controllable dimensions, crystal structure and chemical composition, are obtained [4-7].

In particular, magnetic particles with sizes between 1 nm and 100 nm are useful for the production of magnetic nano fluids [1, 7, 8]. However, micrometer sized particles are used in the production of magnetorheological suspensions [10]. They are known as *smart fluids* [11], and are widely used in mechanical vibration dampers [12], clutches [13], cancer treatment trials [14] etc.

A special class of microparticles are cavitational or hollow ones, such as microspheres [9, 16-18], macrospheres [19], microtubes [20, 21] and microparticles with octopus shape [23]. The later ones are formed from a central core, out of which are branched out ligaments in the same plane. All these particles are also known as *container microparticles* since the useful substances are adsorbed/absorbed inside them. The *containers* can be fixed in predetermined positions of interest, through an external magnetic field. For example, FC-4 type microparticles are obtained by processing mixtures of graphite (powder) and Fe_xO_z in argon plasma jet [24]. The presence of carbon nano-microtubes on iron microparticles represents an adsorbent medium for chemotherapy [24] or it may be a possible way for detoxification of body fluids [25]. Iron microspheres with active substances inside are useful in the treatment of tumors [26, 27], implants protection [28], radiotherapy [29] etc.

On another hand, by dispersing magnetic nano-microparticles in liquid polymers (natural rubber, silicone rubber etc.) followed by polymerization in a mixture with a suitable catalyst, with or without a magnetic field, one obtains magnetorheological elastomers [30-32] with various applications [33, 34].

Following this line of research, in this paper we will present the production process and formation mechanisms of iron nano-microparticles in argon plasma.

Theoretical background

For plasma temperatures (T_{oi}) of about 10000 K, the solid metal iron in the form of wire or rod is instantly transformed into vapors. The molar concentration of iron vapor is:

$$C_{oi} = \frac{p_i}{RT_{oi}}, \quad (1)$$

where $R=8.314 \text{ J}/(\text{mol K})$ is the universal constant of the ideal gas, and p_i is vapors pressure. The later depends on T_{oi} according to

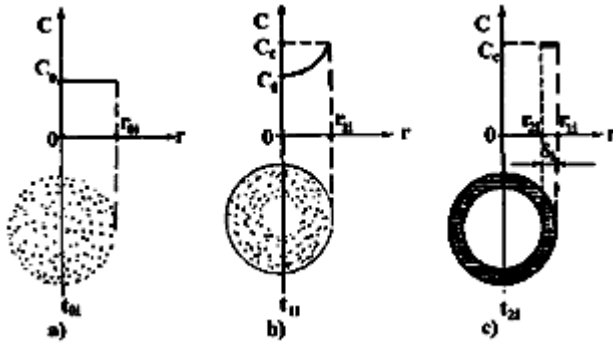
$$p_i = p_{oi} e^{\frac{\Delta L_v}{R} \left(\frac{T_{oi}}{T_b} - 1 \right)}, \quad (2)$$

where ΔL_v is the latent heat of vaporization and p_{oi} is the vapor pressure at temperature T_b .

The movement of gas-vapor mixture is not stable. Inside plasma jet are formed regions with entities containing vapor, divided by regions with gases. If $v_0 \eta \ll \Gamma_{Fe}$, where v_0 is the plasma jet velocity, η is the dynamic viscosity of plasma, and Γ_{Fe} is the surface tension of iron vapors, then the entities defined above are in the form of spheres. If

$v_0 \eta \ll \Gamma_{Fe}$, tubes containing mixtures of argon with iron vapors are formed, which are separated from each other by argon. At the initial moment (t_{oi}), we consider that r_{oi} is the sphere/tube radius formed by the gas and vapors (fig. 1a). Then, according to ideal gas law, we can write:

* email: eanitasro@gmail.com



$$r_{0i} = \left(\frac{3 m_{vi}}{4\pi \mu C_0} \right)^{\frac{1}{3}}, \quad (3)$$

where μ and m_{vi} are the molar mass and respectively the iron vapor mass.

The spheres and tubes consisting of gas and vapors are moving with the velocities of the plasma jet. At t_{1i} , the sphere/tube interface reaches the point characterized by temperatures equal with the temperatures of *dew point*. Then the sub-cooling of the gas-vapor system is $\Delta T \equiv T_0 - T_1$ where T_1 is the *dew point* temperature. Then, at constant pressure the interface turns into a liquid membrane with the concentration of nano-microparticle's sprouts in the liquid phase given by:

$$C_c = C_0 e^{\frac{\Delta E}{R\Delta T}}, \quad (4)$$

and with membrane's radius given by:

$$r_{1i} = r_{0i} \left(\frac{T_1}{T_0} \right)^{1/3}, \quad (5)$$

where ΔE is the activation energy of the iron vapor condensation.

Inside the sphere/tube of radius r_{1i} (fig. 1b) a temperature gradient occurs with a direction towards the liquid membrane. The vapor volume element is placed on the membrane. It takes place a non-steady vapor transport [35] and then another volume element takes its place. The process continues until there is no vapor inside the sphere and the membrane's thickness increases up to $\delta_i = r_{1i} - r_{2i}$ (fig. 1c). At ambient temperatures, particles in the form of nano-microspheres/tubes are formed, the conditions for their formation being fulfilled. Due to the viscosity of gas-vapor mixture, the fluid spheres encounters a resistance. At a given point, and for a short period, the fluid sphere becomes immobile. At this moment, the hydrodynamic spectrum of the liquid medium surrounding the sphere consists of a circular motion around an obstacle, combined with a movement produced by a punctual vortex (fig. 2).

The punctual vortex is produced around a circle resulted from the intersection between the sphere and the plane of movement of the liquid medium. Then, the characteristic function of the medium is [35]:

$$f(r, \theta) = v_\infty \left(r + \frac{R^2}{r} \right) \cos \theta + \frac{\Gamma}{2\pi} \theta + i \left(v_\infty \left(r - \frac{R^2}{r} \right) \sin \theta - \frac{\Gamma}{2\pi} \ln r \right) \equiv \phi(r, \theta) + i \psi(r, \theta), \quad (6)$$

from which we obtain the potential's velocities:

$$\phi(r, \theta) = v_\infty \left(r + \frac{R^2}{r} \right) \cos \theta + \frac{\Gamma}{2\pi} \theta, \quad (7)$$

and the current function

Fig. 1. The steps of microspheres formation in plasma. a) t_{0i} - the moment of gas-vapor sphere formation, with radius r_{0i} . b) t_{1i} - the moment of liquid membrane formation, with radius r_{1i} . c) the moment of microsphere formation with inner radius r_{2i} and wall thickness $\delta_i = r_{1i} - r_{2i}$. Here, C_0 is the molar concentration of the vapors, C_{ci} is the critical concentration of nano-microparticles in (sprouts) in liquid phase and O_i is the coordinate axis [35].

$$\psi(r, \theta) = v_\infty \left(r - \frac{R^2}{r} \right) \sin \theta - \frac{\Gamma}{2\pi} \ln r, \quad (8)$$

where (r, θ) are polar coordinates, v_∞ is the velocity of the fluid medium, R is the radius of the sphere and Γ is the velocity circulation. The differential equation of current lines is $d\psi(r, \theta) = 0$. Then, using eq. (6) we obtain

$$\Psi(r, \theta) = c, \quad (9)$$

where c is a constant. By using eq. (9), and for $r = R$ we obtain $\Psi(r, \theta) = -r/(2\pi) \ln R$. Further, by using eq. (6) we obtain the velocities of the complex movement of the fluid around the sphere:

$$\omega = v_\infty \left(1 - \frac{R^2}{r^2} \cos 2\theta \right) - \frac{\Gamma}{2\pi r} \sin \theta + i \left(-\frac{v_\infty R^2}{r^2} \sin 2\theta + \frac{\Gamma}{2\pi r} \cos \theta \right) \quad (10)$$

which allows us to write the velocities of the fluid medium along Ox axis such as:

$$u = v_\infty \left(1 - \frac{R^2}{r^2} \cos 2\theta \right) - \frac{\Gamma}{2\pi r} \sin \theta, \quad (11)$$

and the velocities of the fluid medium along Oy axis, as:

$$v = -\frac{v_\infty R^2}{r^2} \sin 2\theta + \frac{\Gamma}{2\pi r} \cos \theta. \quad (12)$$

By using $r = R$ in eqs. (11) and (12) we obtain

$$u = v_\infty (1 - \cos 2\theta) - \frac{\Gamma}{2\pi R} \sin \theta, \quad (11)$$

$$v = -v_\infty \sin 2\theta + \frac{\Gamma}{2\pi R} \cos \theta, \quad (12)$$

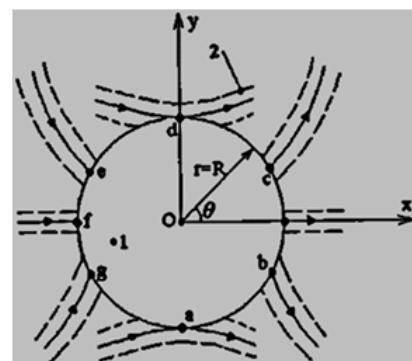


Fig. 2. Fluid sphere.

1 - Microsphere and/or a drop. 2 - a cylinder with gas and vapor. a, b, ..., g - stagnation points for the gas-vapor mixture, R is the radius Oxy is a Cartesian system of coordinates, r and θ are polar coordinates [35]

and thus

$$|\omega| \equiv \sqrt{u^2 + v^2} = 2v_\infty \sin \theta - \frac{\Gamma}{2\pi r}. \quad (13)$$

The last equation shows that the stagnation points of the fluid medium on the circle with radius $r = R$ are given by:

$$\sin \theta = \frac{\Gamma}{4\pi v_\infty R} = \frac{\alpha}{4\pi R}, \quad (14)$$

where we have denoted $\alpha = \Gamma/v_\infty$.

Due to velocity distribution of the fluid medium on the circular section of the plasma jet, to the intermittent introduction of the metal in plasma, and due to the molar concentration of the vapor, which is small compared to the molar density of the gas-vapor mixture, the quantity α will be given by:

$$\alpha = 4\pi R n, \quad (15)$$

where the numbers $n = -1, -\frac{1}{2}, 0, \frac{1}{2}, 1$ are the discretization factors.

By denoting $y = R \sin \theta$ and using eq. (15) we obtain

$$y = \frac{\Gamma}{4\pi v_\infty} = \frac{\alpha}{4\pi} \text{ or } y = nR, \quad (16)$$

which shows, that there exist eight stagnation points of the fluid medium on the circle with radius $r = R$ (fig. 2). With respect to these points, the current lines and the cylinders that contain them, take the following positions in figure 2: at points a) and d) they are tangent to the circle, at points b) and c) their origin is on the sphere, and they sting the sphere at points e) and g). These stagnation centers form the growth centers of the nano-microtubes.

Experimental part

Materials and methods

The experimental setup used for producing microparticles using plasma processes is shown in figure 3. It consists of a plasma generator connected to a power source for the plasma arc transferred, and to the ballast resistance, for the pilot plasma arc. The supply with argon is performed from the argon storage. Cooling the plasma generator is done with tap water. The advance of the rod electrode is realized by the system of material displacement connected to an auto-transformer through a separator.

The current intensity is fixed and the plasma is primed on the rod electrode connected to the positive terminal of the electric source (fig. 4). By modifying the main parameters of the plasma arc transferred (electric current intensity, argon flow and velocity of material displacement) one obtains velocities v_0 of plasma jet, and the temperatures



Fig. 3. Experimental setup used for production of iron microparticles in plasma. 1 - plasma generator (intensity of electric current is max 600 A_c), 2 - rectifier bridge, 3 - power source (max 110 A_c), 4 - power resistance (2Ω/3kW), 5 - autotransformer, 6 - separator transformer, 7 - power supply, 8 - advance system, 9 - argon storage under pressure (130 bar).

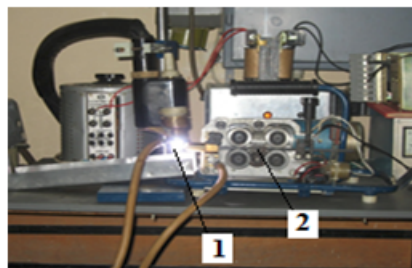


Fig. 4. Electric arc plasma primed on the rod electrode. 1 - argon plasma, 2 - carbon steel rod

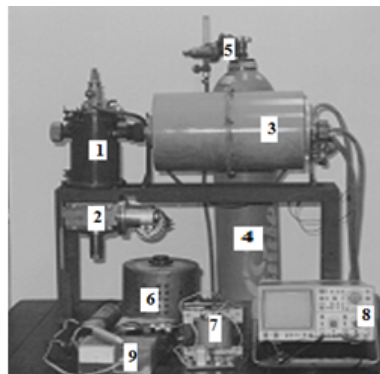


Fig. 5. Overview of the experimental setup generating magnetisable nanoparticles. 1 - plasma chemical generator block, 2 - system for material displacement, 3 - nanoparticles collection site, 4 - argon cylinder, 5 - spherical valve flowmeter, 6 - autotransformer, 7 - separation transformer with bridge rectifier, 8 - oscilloscope, 9 - photodiode-based rotameter



Fig. 6. Plasma generator after spraying the iron rod. 1 - Iron rod, 2 - Plasma generator block.

of argon plasma which allow metal spraying. Submicron particles give exothermal reaction in contact with oxygen in the air and thus their production is performed using setups with controlled storage environment (fig. 5).

Plasma is primed in the plasmochimical generator block in argon medium, on the metal rod connected to the positive terminal of the current source. At plasma priming, the metal bar is consumed by spraying, as shown in figure 6.

A second important way of generating iron particles is the use of a welding head of tungsten-inert gas connected to a power source (item 3 in fig. 5) by adjusting the advance velocity of the electrode (carbon steel rod) connected to the positive terminal of the same source current. The melt is sprayed under the dynamic pressure of the plasma jet (fig. 7).

Results and discussions

The experimental model in figure 4, whose overall configuration is shown in figure 8 is used for production of particles in plasma.

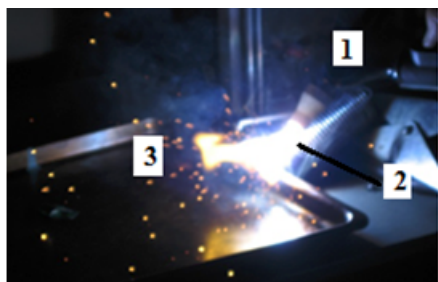


Fig. 7. Spraying the carbon steel rod in plasma of tungsten-inert gas arc. 1 - welding head, 2 - plasma jet, 3 - drops of metal sprayed in the argon plasma

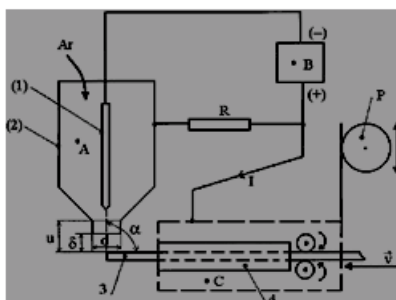
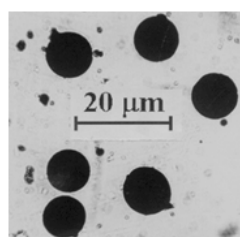
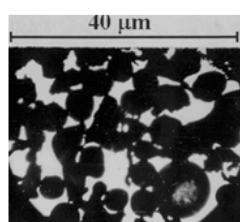


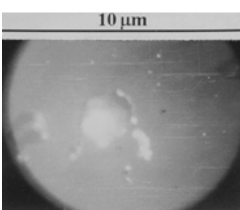
Fig. 8. Experimental setup. A - plasma generator, B - power source, C - advance wire block, 1 - tungsten electrode, 2 - nozzle, 3 - wire electrode, 4 - contact nozzle, R - power resistor ($2\Omega/3kW$), P - positioning system, I - electric current intensity through the discharge, U - electric arc voltage, α - wire-plasma incidence angle, d - nozzle diameter, Ar - plasma gas, v - wire advance velocity, δ - wire nozzle distance [35 - 37]



a)

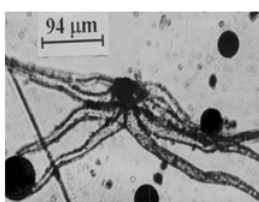


b)

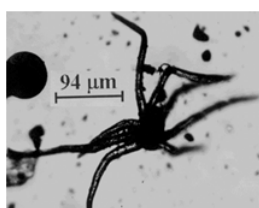


c)

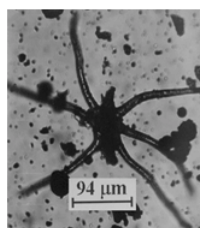
Fig. 9. Shapes and dimensions of iron micro particles: a) micro particles, microspheres, and melted iron mass; b) micro particles and microspheres; c) microsphere with pores.



a)

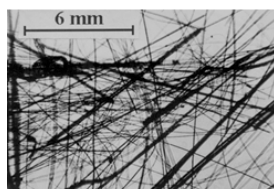


b)

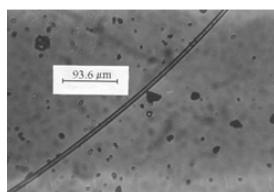


c)

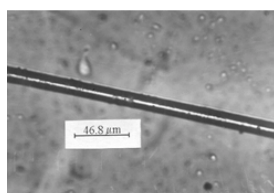
Fig. 10. Iron micro particles with ligaments formed by a central core from which the micro tubes branch out [35 - 37].



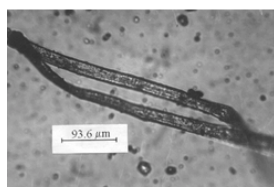
a)



b)



c)



d)

Fig. 11. a) Fibers. b), c), d) Iron micro tubes.

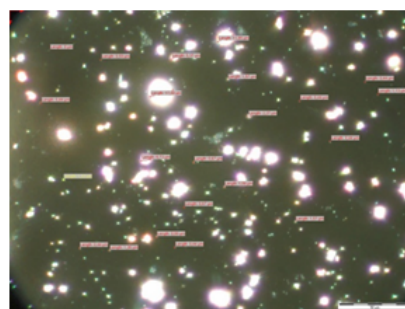


Fig. 12. micro particles by tungsten inert gas method (argon flow: 16 L/min; current intensity: 80 A_{dc})

\Rod diameter is $d_c = 3 \cdot 10^{-3} \text{ m} \pm 10\%$. The chemical composition of steel (in mass percentage) is: C: 0.19, Mn: 10.85, P: 0.045, S: 0.045, Si: 0.40 and Fe: 88.47. The plasma generator has the nozzle with diameter $2 \cdot 10^{-3} \text{ m}$. The distance between the nozzle of the plasma generator and the rod is fixed at $\delta = 6 \cdot 10^{-3} \text{ m}$ and $\alpha = \frac{\pi}{2} \text{ rad}$. The intensity of the electric current through the plasma arc transferred on the electrode rod is $I = 175 \text{ A}_{dc} \pm 10\%$. Rod velocity v and argon flow D , are quantities that change during experiment. For $v = 1.05 \cdot 10^{-3} \text{ m/s}$ and $D = 0.35 \cdot 10^{-3} \text{ m}^3/\text{s}$, rod parts are melted and transported, in a continuous flow, by the plasma gas. Then, through solidification, a solid mass is obtained. Growing the advance velocity of the rod at $v = 1.10 \cdot 10^{-3} \text{ m/s}$ it results iron micro particles and solidified melt (fig. 9 a).

The advance velocity of the rod is maintained at the same value. Instead, we grow the argon flow at $1.00 \cdot 10^{-3} \text{ m}^3/\text{s}$. It results 95 % iron micro particles (fig. 11b) from the total number of particles. Optical microscopy, shows that some micro particles have pores as it is shown in figure 9c. Analyzing a number of about 450 particles, 35 % are microspheres with pores. The medium microsphere



Fig. 13. Shapes and dimensions of the iron nanotubes (intensity electric current by discharger is 300 A_{cc}, argon flow is 0.00026 m³/s and the distance generator-carbon steel bar is 0.005 m)

has the diameter 10 mm and the wall thickness 0.75 μm. At $v = 1.25 \times 10^{-3}$ m/s and $D = 0.65 \times 10^{-3}$ m³/s one obtains, micro particles, microspheres, and also about 15% micro particles with a central core (microspheres) from which tentacles branches out in the same plane. In figure 10 we can observe that the tentacles are empty inside. Their average dimension are for the core (diameter: 12 μm and wall thickness: 0.5 μm) and for the tentacles (length: 188 μm, equivalent diameter: 2 μm, wall thickness: 0.35 μm). At $n = 1.15 \times 10^{-3}$ m/s and $D = 0.75 \cdot 10^{-3}$ m³/s, the melt moves in the plasma on continuous parallel trajectories. After the solidification of the melt are obtained fibers as shown in figure 11a. Viewed at the optical microscope, they appear in the form of tubes of shape and dimensions shown in figures 11b to 11d.

The average micro tube has a length of 100 μm, diameter 27.64 μm and the wall thickness 0.25 μm. Hollow micro particles have their surface covered with Fe₃O₄. The presence of Fe₃O₄ is caused by the traces of oxygen from the technical argon. A number of 450 hollow particles are analyzed. The radius of the hollow micro particles is measured at the optical microscope. The volume occupied by the metal is determined, then the concentration of iron is calculated for each species of micro particles. Thus, for the microspheres, the volume concentration of Fe is 12%, for microtubes is 35% and for microparticles with ligaments is 10%.

By tungsten inert gas process (fig. 7) micro particles are generated with shapes and dimensions as shown in figure 12. The dimension of the particles is between 0.44 μm and 17.09 μm. With the magnetometer YSM-880 (Physica) the magnetization curve of the 178 mg powder is raised [35, 37]. The surface of hysteresis is zero and magnetization of saturation is installed at intensities of the magnetic field 840kA/m and has the value $M_s = 0.0725 \text{ Am}^2/\text{g}$ [35, 37, 38].

Using the installation described in figure 5, by vaporization of the carbon steel bar in the transferred plasma arc (fig. 7), iron nanotubes are obtained with shapes shown in figure 13 and with dimensional distributions shown in figure 14.

Conclusions

Iron powder with nano-micrometer dimensions can be produced by the metallic solid spraying in the transferred arc plasma and in the discharge tungsten-inert-gas. The granulation of the iron powder depends on the velocity distribution over the cross section of the plasma jet and also on the advance velocity of the material.

The obtained iron powder is polydisperse and magnetisable. By adjusting the main parameters of the electrical discharge, one obtains hollow particles (microspheres, porous microspheres, microtubules and

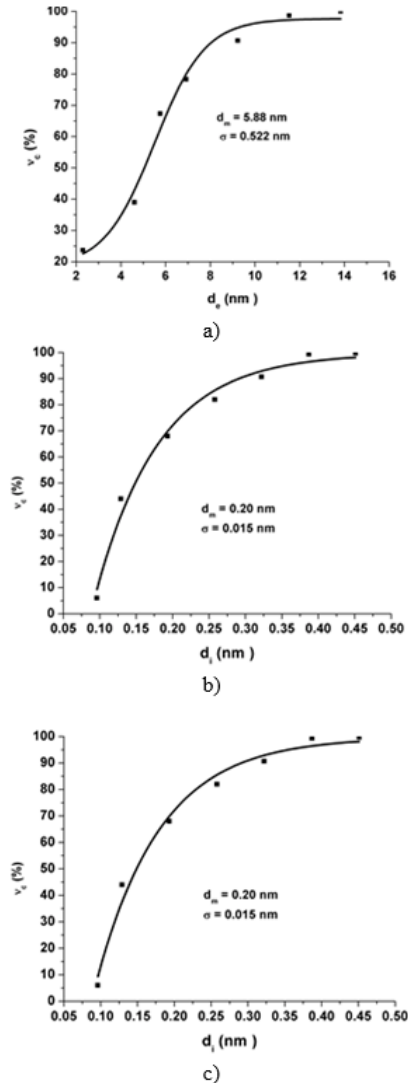


Fig.14. Cumulated size frequency function of: a) outer diameter d_o ; b) inner diameter d_i ; c) the length of nanotubes L_c .

micro particles with a central core) from which the microtubes in the form of ligaments branches out [39, 40]. To decrease the polydispersity of the powder it is necessary to assure uniform velocities in the argon plasma jet.

Collection of iron powder inside a convention hall with gas mixtures (Ar + H₂, Ar + N₂) can reduce the rate of oxidation of the iron particles.

By using solid metal spraying in plasma and in the inert gas environment, iron nanotubes are obtained.

Acknowledgments: The authors thank to their colleagues from University Politehnica of Timisoara for assistance relating to optical microscopy, raising the magnetization curves, hysteresis and also for the Rontgen analysis of the particles obtained by the plasma methods.

References

1. I. BICA, D. BICA, The obtaining of the magnetic liquids, Physics Monographs, vol.12, The Printing House of the University of Timi^ooara, Timi^ooara, 1992;
2. I. BICA, The obtaining of magnetorheological suspension based on silicon oil and iron particles, Mat. Sci. Eng., B **98**, 2 (2003), 89-93;
3. I. BICA, Mesoscopic particles, Editura Mirton, Timisoara, 1997;
4. I. BICA, Nanoparticle production by plasma, Mat. Sci. Eng., B **68** (1999), 5-9;
5. M. UDA, production of ultrafine metal and alloy powders of hydrogen thermal plasma, Nanostructured Materials, **1**, (1992), 101-106;
6. Y. KIHUCHI, F. MATSUDA, H. IKEDA, Effect of Ar and He Pressure on the Formation of the Metal Fine Powder by TIG and MIG Arc melting Process, Transactions of JWRI, **22**, 2 (1993), 249-256;

7. I. BICA, I. MUSCUTARIU, Obtaining nanoparticles from iron and graphite in argon plasma, *Rev. Metal. Madrid*, **32**, 5, (1996), 298-302;
8. I. NAKATANI, T. FURUBAYASHI, Iron - nitride magnetic fluids prepared by plasma CVD technique and their magnetic properties, *J. Magn. Magn. Mater.*, **85** (1993), 11-13;
9. I. BICA, Iron microspheres generation in argon plasma jet, *Mat. Sci. Eng., B*, **88**, (2002), 107-109;
10. I. BICA, The obtaining of magnetorheological suspensions based on silicon oil and iron particles, *Mat. Sci. Eng., B*, **98**, 2, (2003), 89-93;
11. K. WORDEN, W. A. BULLOUGH, J. HAYWOOD, *Smart Technologies*, World Scientific, London, 2003;
12. I. BICA, Damper with magnetorheological suspension, *J. Magn. Magn. Mater.*, **241**, (2002), 196-200;
13. I. BICA, Magnetorheological suspension electromagnetic brake, *J. Magn. Magn. Mater.*, **270**, 3, (2004), 321-326;
14. G. FLORES, R. SHENG, J. LIU, Medical Applications of Magnetorheological Fluids-A Possible New Cancer Therapy. In: „Proceed. Of the 7th Int. Conf. on ERF and MRS”, Ed. R. Tao, World Scientific, Singapore, (2000), pp. 716-726;
15. I. BICA, Cavitation micro-particles: plasma mechanisms formation, *Romanian Reports in Physics*, **57**, 1, (2005), 79-84;
16. I. BICA, Obtaining of Microspheres in Plasma: Theoretical Model, *Mat. Sci. Eng. B*, **77**, (2000), 293-296;
17. I. BICA, On the mechanisms of iron microspheres formation in argon plasma jet, *J. Magn. Magn. Mater.*, **257**, (2003), 119-125;
18. I. BICA, Pore formation by plasma procedure, *Mater. Sci. Eng. A*, **303**, 1-2, (2005), 191-195;
19. I. BICA, Formation of Iron Macrospheres in Plasma, *Plasma Chemistry and Plasma Processing*, **25**, 2, (2005), 121-135;
20. I. BICA, Obtaining SiO₂ Microtubes in Plasma Jet, *Mat. Sci. Eng. B*, **96**, (2001), 269-171;
21. I. BICA, Some mechanisms of SiO₂ microtubes formation in plasma jet, *Plasma Chemistry and Plasma Processing*, **23**, 1, (2003), 175-182;
22. I. BICA, Formation of iron microtubes in argon plasma, *J. Magn. Magn. Mater.*, **270**, 1-2, (2004), 321-326;
23. I. BICA, Some mechanisms for the formation of octopus shaped iron micro-particles, *J. Magn. Magn. Mater.*, **279**, 2-3, (2004), 289-298;
24. A. A. KUZNETSOV, A. R. HARUTYUNYAN, E. K. DOBRINSKY, V.I. FILIPOV, A.G. MALENKOV, A.F. VANIN, O.A. KUZNETSOV, Ferro-Carbon Particles: Preparation and Clinical Applications. In: „Scientific and Clinical Applications of Magnetic Carriers”, edited by U.O. Häfeli, W. Schütt, J. Teller, M. Zborowsky, Plenum Press, New York and London, (2001), pp.379-390;
25. M. V. KUTUSHOV, A.A. KUZNETSOV, V.I. FILIPOV, O.A. KUZNETSOV, New Method of Biological Fluid Detoxification Based on Magnetic Adsorbents, In: *Scientific and Clinical Applications of Magnetic Carriers*, edited by U.O. Häfeli, W. Schütt, J. Teller, M. Zborowsky, Plenum Press, New York and London, (2001), pp. 391-398;
26. Sh. K. PULFER, J. M. GALLO, Targeting Magnetic Microspheres to Brain Tumors, In: *Scientific and Clinical Applications of Magnetic Carriers*, edited by U Häfeli, W. Schütt, J. Teller, M. Zborowsky, Plenum Press, New York and London, (2001), pp. 445-456;
27. A. ST. LULBE, CH. BEGERMANN, Selected Preclinical and First Clinical Experiences with Magnetically Targeted - Epidoxorubicin in Patients with Advanced Solid Tumors, In: *Scientific and Clinical Applications of Magnetic Carriers*, edited by U HÄFELI, W. SCHÜTT, J. TELLER, M. ZBOROWSKY, Plenum Press, New York and London, (2001), pp. 457-480;
28. S. YA. MAKHMUDOV, A.A. KUZNETSOV, V. I. FILIPOV, Magnetically Guided Drug Transport for the Prophylaxis of Pathological Conditions and the Protection of Implants, In: *Scientific and Clinical Applications of Magnetic Carriers*, edited by U Häfeli, W. Schütt, J. Teller, M. Zborowsky, Plenum Press, New York and London, (2001), pp.495-500;
29. U. O. HAFELI, G. J. PAUER, W. K. ROBERTS, J. L. HUMM, R. M. MACKLIS, Magnetically Targeted Microspheres for Intracavitary and Intraspinal Y-90 Radioterapy, In: „Scientific and Clinical Applications of Magnetic Carriers”, edited by U Häfeli, W. Schütt, J. Teller, M. Zborowsky, Plenum Press, New York and London, (2001), pp. 501-516;
30. I. BICA, E.M. ANITAS, M. BUNOIU, B. VATZULIK, I. JUGANARU, Hybrid magnetorheological elastomer: influence of magnetic field and compression pressure on its electrical conductivity, *J. Ind. Eng. Chem.*, **20** (2014), 3994-3999;
31. I. BICA, E.M. ANITAS, L.M.E. AVERIS, Tensions and deformations in composites based on polyurethane elastomer and magnetorheological suspension: Effects of the magnetic field, *J. Ind. Eng. Chem.*, **28**, (2015) 86-90;
32. M. BUNOIU, I. BICA, Magnetorheological elastomer based on silicone rubber, carbonyl iron and Rochelle salt: Effects of alternating electric and static magnetic fields intensities, *J. Ind. Eng. Chem.*, **37**, (2016) 312-318;
33. I. BICA, Magnetorheological elastomer-based quadrupolar element of electric circuits, *Mat. Sci. Eng.: B*, **166** (2010), 94-98;
34. I. BICA, Magnetoresistor sensor with magnetorheological elastomers, *J. Ind. Eng. Chem.*, **17** (2011), 83-89;
35. I. BICA, *Fizica si tehnologia materialelor in plasma*. Editura Mirton, Timisoara, 2006;
36. I. BICA, Cavitation micro-particles: plasma formation mechanisms, *Rom. Rep. Phys.*, **57** (2005), 79-84;
37. I. BICA, M. BUNOIU, L. CHIRIGIU, M. SPUNEL, I. JUGANARU, Cavitation Iron Microparticles Generation by Plasma Procedures for Medical Applications, *Annals of West University of Timisoara-Physics*, **56** (2012), 9-14;
38. I. BICA, Production of iron nanotubes in plasma, *J. Ind. Eng. Chem.*, **14**, (2008) 230-235.
39. E. C. STANCIULESCU, C. G. PISOSCHI, G. RAU, A. M. ANDREI, M. BANITA, Proteasome inhibition: recent advances in antitumoral therapy, *Farmacia*, **62** (2), (2014), p. 245-253
40. G. D. MOGOSANU, A. PINTEA, L. E. BEJENARU, C. BEJENARU, G. RĂU, H. POPESCU, HPLC analysis of carotenoids from *Senecio vernalis* and *S. jacobaea* (Asteraceae), *Farmacia*, **57** (6) (2009), p. 780-786

Manuscript received: 14.12.2016